Supporting information

In-situ Formation of $NaTi_2(PO_4)_3$ Cubes on Ti_3C_2 MXene for Dual-mode Sodium Storage

Qi Yang[1], Tianpeng Jiao[1], Mian Li[2], Youbing Li[2], Longtao Ma[1], Funian Mo[1], Guojin Liang[1], Donghong Wang[1], Zifeng Wang[1], Zhaoheng Ruan[1], Wenjun Zhang[1], Qing Huang[2]*, Chunyi Zhi[1, 3]**

[1] Department of Materials Science and Engineering, City University of Hong Kong, 83 Tat Chee Avenue, Hong Kong SAR, China

[2] Engineering Laboratory of Specialty Fibers and Nuclear Energy Materials, Ningbo Institute of Materials Engineering and Technology Chinese Academy of Science, Ningbo, Zhejiang 315201, China

[3] Shenzhen Research Institute, City University of Hong Kong, Nanshan District, Shenzhen 518057, PR China.

**E-mail: apwjzh@cityu.edu.hk; huangqing@nimte.ac.cn.; c.y.zhi@cityu.edu.hk*

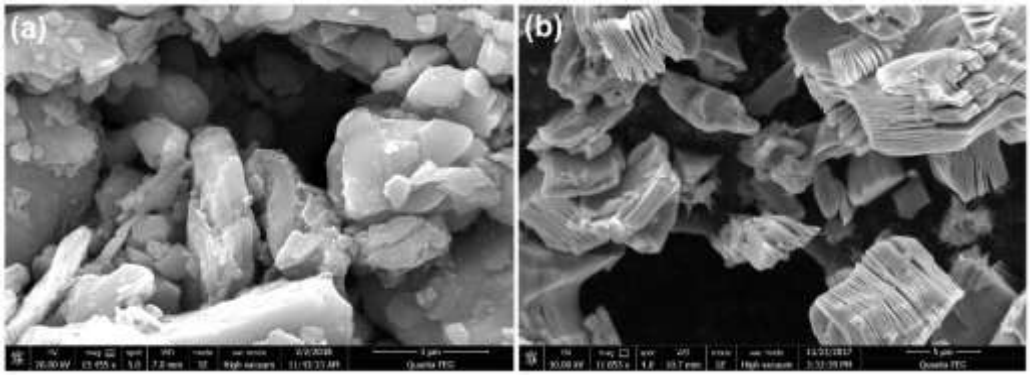

Figure S1. SEM images of layered Ti_3AlC_2 MAX phase (a) and Ti_3C_2 Mxene nanosheets (b) fabricated by a mature HF etching method.

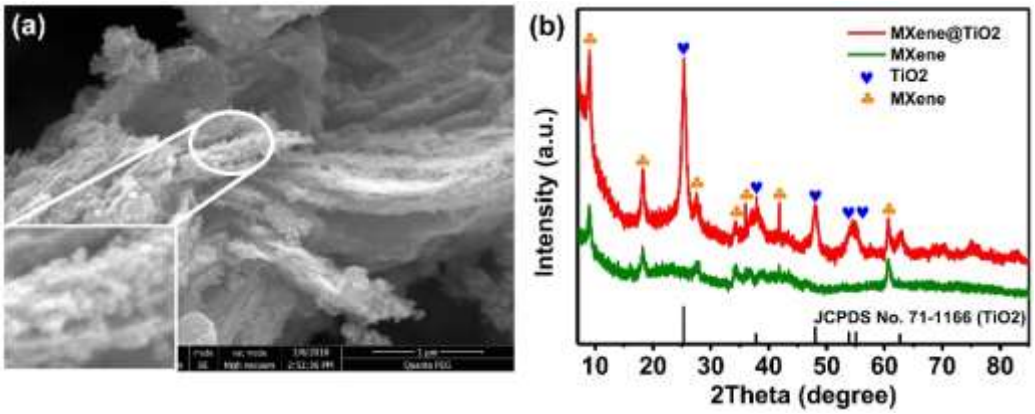

Figure S2. SEM image (a) and XRD pattern (b) of MXene@TiO_2 prepared by oxidizing MXene using H_2O_2 without adding sodium acetate trihydrate and phosphoric acid. The SEM image reveals that large amounts of TiO_2 nanoparticles in-situ appear in nanogaps between the adjacent MXene nanosheets. The coexistence of characteristic peaks of both MXene and TiO_2 in the XRD pattern further verifies the formation of TiO_2 on MXene nanosheets.

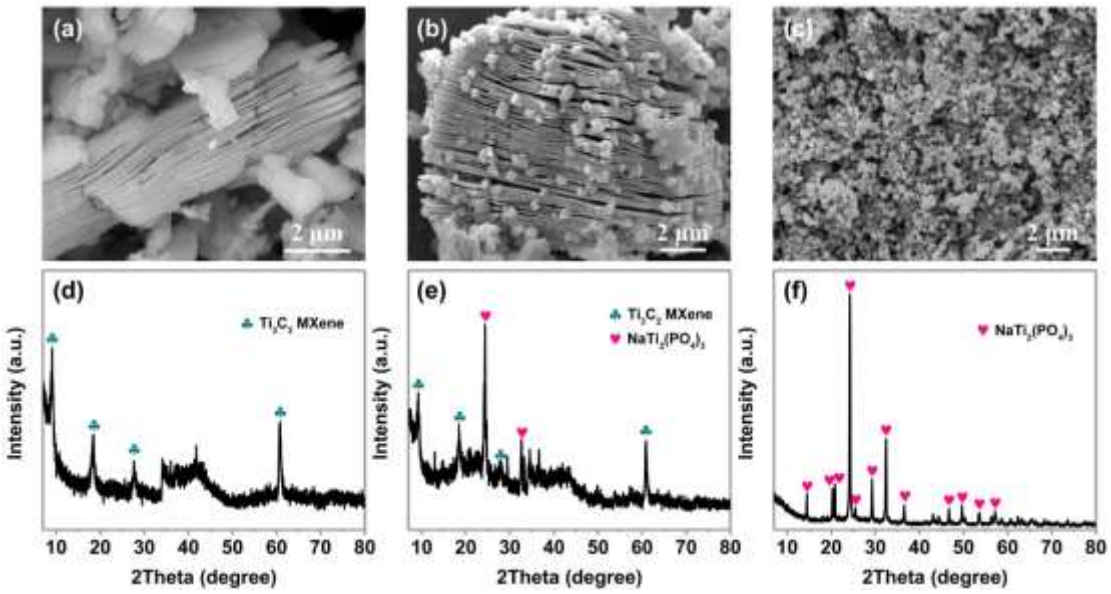

Figure S3. Morphology and composition transition from neat MXene (zero transformation rate) to MXene@NTP-L (low transformation rate) and NTP-C (100% transformation rate). SEM image and XRD data of neat MXene (a, d); SEM image and XRD data of MXene@NTP-L (b, e); SEM image and XRD data of neat NTP (c, f).

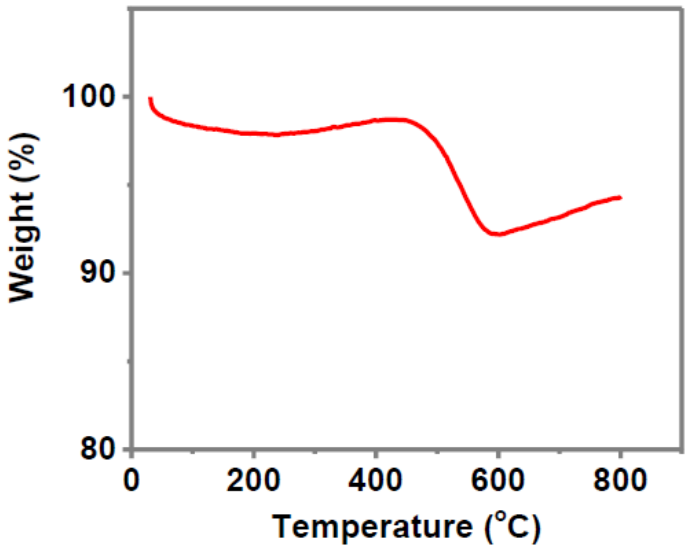

Figure S4. Thermal gravimetric analysis of MXene@NTP-C in oxygen, which suggests that the carbon layer accounts for about 8 wt% of the whole weight of MXene@NTP-C. The tiny increase of weight after 600 ^{o}C is attributed to the oxidation of Ti_3C_2 MXene by oxygen.

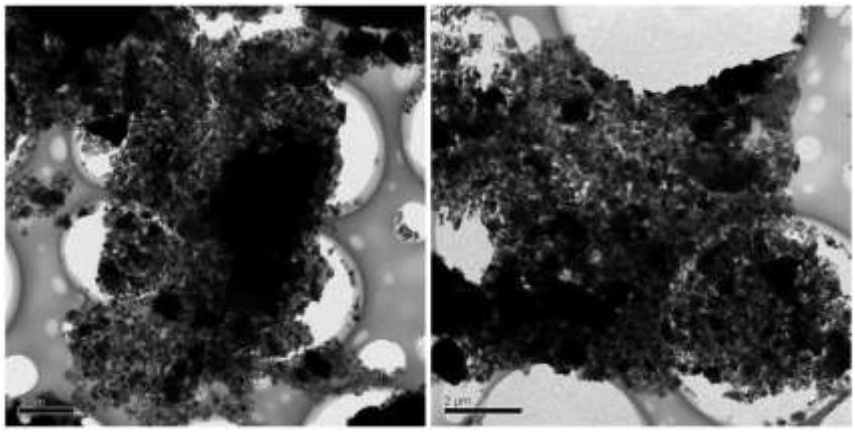

Figure S5. TEM images of MXene@NTP-C nanohybrids with a sheet-like topological structure decorated by enormous $NaTi_2(PO_4)_3$ cubes. It should be noted that the ultrasonic exfoliation must be conducted to decrease the thickness of MXene@NTP-C hybrids before TEM observation.

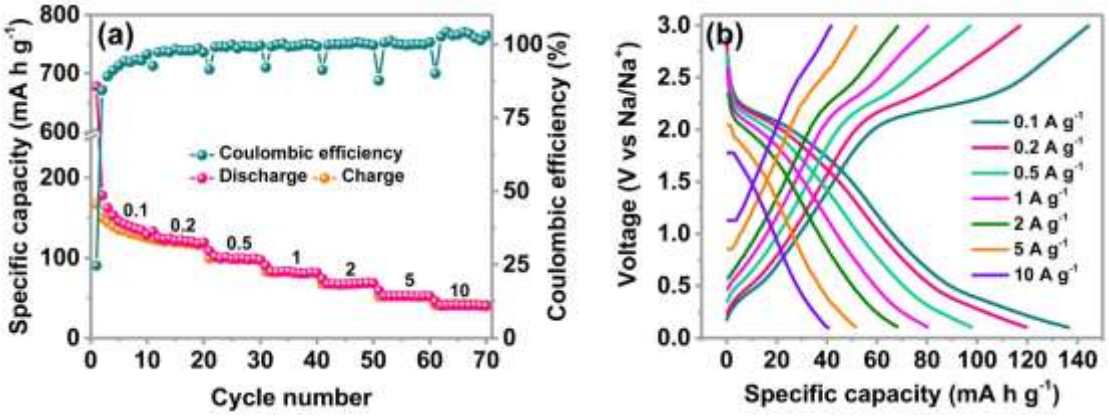

Figure S6. Rate capabilities (a) and the corresponding discharge-charge curves (b) of MXene@NTP without carbon coating. It is obviously that MXene@NTP showed a lower specific capacities at current densities of 0.1-10 A g^{-1}. This phenomena can be illustrated by the shortened voltage platforms caused by the inferior conductivity without carbon coating.

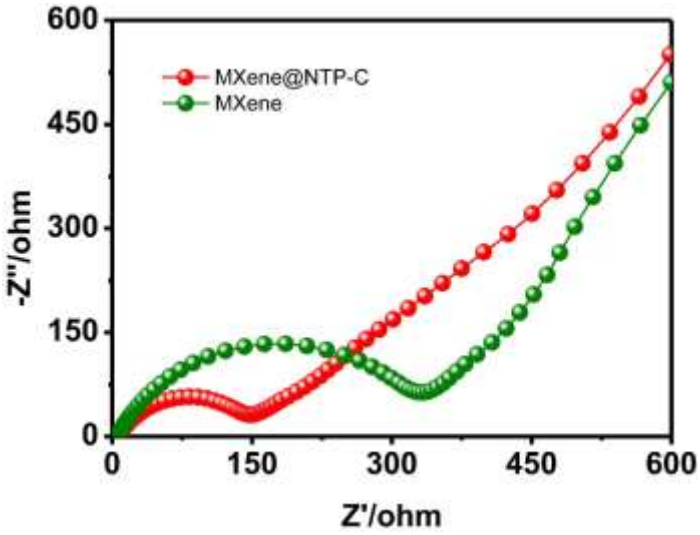

Figure S7. Nyquist plots of MXene@NTP-C and the original MXene, and their expanded high-frequency regions. The semicircle with a much smaller radius at the high-frequency region suggests that MXene@NTP-C electrode exhibits much lower charge transfer resistance compared to that of MXene.

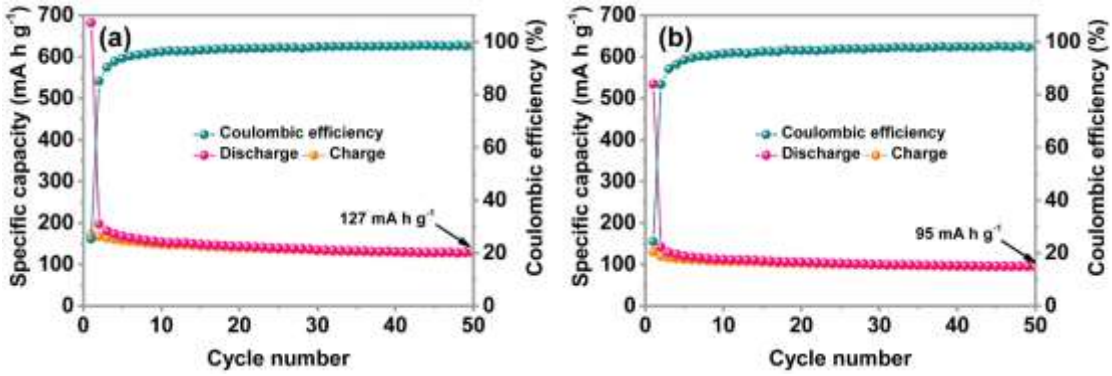

Figure S8. Cycle performance at the current density of 0.1 A g^{-1} of NTP-C (neat $NaTi_2(PO_4)_3$) (a) and the mixture of MXene and NTP-C (b). Both NTP-C and the simple mixture show lower specific capacities than MXene@NTP-C

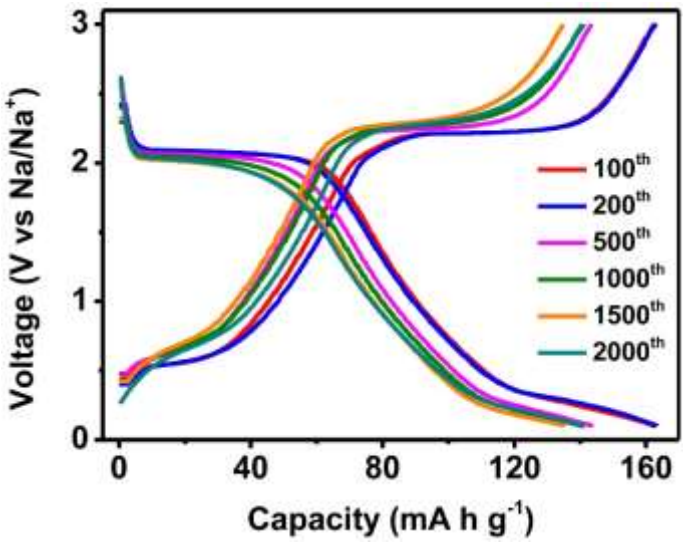

Figure S9. Discharge/charge profiles of MXene@NTP-C from the 100th to the 2000th cycle at a current density of 1A g^{-1}.

Table S1. Comparison of current density, specific capacity, and lifespan between this work and the related ones in previous literature.

Sample	Current density (mA g^{-1})	Specific capacity (mA h g^{-1})	Lifespan (cycles)	Reference
MXene@NTP-C	1,000	143	2,000	This work
	5,000	109	10,000	
$NaTi_{1.5}O_{8.3}$ nanoribbons	200	136	150	Ref. [1]
$Na_2Ti_3O_7$ nanosheets	1,000	130	1,000	Ref. [2]
$Na_2Ti_3O_7$ nanotubes	354	108	100	Ref. [3]
$Na_2Ti_3O_7$/C	178	112	100	Ref. [4]
TiO_2	50	150	600	Ref. [5]
TiO_2/graphene	500	120	4,300	Ref. [6]
B-doped TiO_2	660	150	400	Ref. [7]
N-doped TiO_2	3,350	110	500	Ref. [8]
$Na_{0.23}TiO_2/Ti_3C_2$	2,000	56	4,000	Ref. [9]
Ti_2C MXene	20	142	100	Ref. [10]
Ti_3C_2 MXene	200	68.3	1,000	Ref. [11]

Reference

1. Dong, Y.; Wu, Z. S.; Zheng, S.; Wang, X.; Qin, J.; Wang, S.; Shi, X.; Bao, X. Ti3C2 MXene-Derived Sodium/Potassium Titanate Nanoribbons for High-Performance

Sodium/Potassium Ion Batteries with Enhanced Capacities. *ACS Nano* 2017, 11, 4792-4800.

2. Shengyang, D.; Laifa, S.; Hongsen, L.; Gang, P.; Hui, D.; Xiaogang, Z. Flexible Sodium‐Ion Pseudocapacitors Based on 3D Na2Ti3O7 Nanosheet Arrays/Carbon Textiles Anodes. *Advanced Functional Materials* 2016, 26, 3703-3710.

3. Wang, W.; Yu, C.; Lin, Z.; Hou, J.; Zhu, H.; Jiao, S. Microspheric Na2Ti3O7 consisting of tiny nanotubes: an anode material for sodium-ion batteries with ultrafast charge-discharge rates. *Nanoscale* 2013, 5, 594-599.

4. Yan, Z.; Liu, L.; Shu, H.; Yang, X.; Wang, H.; Tan, J.; Zhou, Q.; Huang, Z.; Wang, X. A tightly integrated sodium titanate-carbon composite as an anode material for rechargeable sodium ion batteries. *Journal of Power Sources* 2015, 274, 8-14.

5. Longoni, G.; Pena Cabrera, R. L.; Polizzi, S.; D'Arienzo, M.; Mari, C. M.; Cui, Y.; Ruffo, R. Shape-Controlled TiO2 Nanocrystals for Na-Ion Battery Electrodes: The Role of Different Exposed Crystal Facets on the Electrochemical Properties. *Nano Letters* 2017, 17, 992-1000.

6. Chen, C.; Wen, Y.; Hu, X.; Ji, X.; Yan, M.; Mai, L.; Hu, P.; Shan, B.; Huang, Y. Na+ intercalation pseudocapacitance in graphene-coupled titanium oxide enabling ultra-fast sodium storage and long-term cycling. *Nature Communications* 2015, 6, 6929.

7. Wang, B.; Zhao, F.; Du, G.; Porter, S.; Liu, Y.; Zhang, P.; Cheng, Z.; Liu, H. K.; Huang, Z. Boron-Doped Anatase TiO2 as a High-Performance Anode Material for Sodium-Ion Batteries. *ACS Applied Materials & Interfaces* 2016, 8, 16009-16015.

8. Ying, W.; Xiaowu, L.; Zhenzhong, Y.; Lin, G.; Yan, Y. Nitrogen‐Doped Ordered

Mesoporous Anatase TiO2 Nanofibers as Anode Materials for High Performance Sodium‐Ion Batteries. *Small* 2016, 12, 3522-3529.

9. Huang, J.; Meng, R.; Zu, L.; Wang, Z.; Feng, N.; Yang, Z.; Yu, Y.; Yang, J. Sandwich-like Na0.23TiO2 nanobelt/Ti3C2 MXene composites from a scalable in situ transformation reaction for long-life high-rate lithium/sodium-ion batteries. *Nano Energy* 2018, 46, 20-28.

10. Wang, X.; Kajiyama, S.; Iinuma, H.; Hosono, E.; Oro, S.; Moriguchi, I.; Okubo, M.; Yamada, A. Pseudocapacitance of MXene nanosheets for high-power sodium-ion hybrid capacitors. *Nature Communications* 2015, 6, 6544.

11. Wang, X.; Shen, X.; Gao, Y.; Wang, Z.; Yu, R.; Chen, L. Atomic-Scale Recognition of Surface Structure and Intercalation Mechanism of Ti3C2X. *Journal of the American Chemical Society* 2015, 137, 2715-2721.